Wear, *122* (1988) 301 - 312

A NEW THREE-DIMENSIONAL NON-CONTACT DIGITAL OPTICAL PROFILER

BHARAT BHUSHAN*

IBM Corporation, Tucson, AZ 85744 (U.S.A.)

JAMES C. WYANT

Optical Sciences Center, University of Arizona, Tucson, AZ 85721 (U.S.A.)

JOHN MEILING

WYKO Corporation, Tucson, AZ 85719 (U.S.A.)

(Received July 29, 1987; accepted September 21, 1987)

Summary

New features of a three-dimensional non-contact digital optical profiler are described. This instrument uses a Michelson interferometer for 1.5X, 2.5X, and 5X objective magnifications, a Mirau interferometer for 10X, 20X, and 40X magnifications, and a Linnik objective for 100X, 150X, and 200X magnifications. The instrument is capable of a lateral resolution of 0.4 μm and a vertical resolution as small as 0.1 nm. The software can calculate various statistical roughness parameters for flat, cylindrical, and spherical surfaces. The radii of cylindrical and spherical surfaces can be measured with high accuracy. Flatness, crown, camber, twist, taper angle, pole-tip gap recession, and edge quality of magnetic slider surfaces can also be measured.

1. Introduction

There are many ways of measuring how the roughness of a surface affects its physical properties. Most of these possibilities have been explored at one time or another [1]. Some methods, because of their inherent disadvantages, have disappeared without trace but there are many that possess possibilities that might merit further investigation today. In some cases, the limitations that prevented their original use have been removed by advances in technology. In other cases, methods that were developed to deal with difficult but infrequent measurement problems have subsequently become of greater practical or economic importance.

*Present address: IBM Almaden Research Center, San Jose, CA 95120, U.S.A.

0043-1648/88/$3.50

Non-contact non-destructive methods of measuring roughness are especially attractive for soft surfaces [2]. In addition, many fundamental problems associated with surface roughness require quantitative information about the surfaces in three dimensions with high vertical and lateral resolutions. In response to these needs, a two- or three-dimensional non-contact optical profiler was developed by Wyant *et al.* [3]. The instrument has been modified to have a wide range of lateral resolutions. Extensive software has been developed to measure various statistical roughness parameters and geometrical parameters of a surface.

2. Description of the optical profiler

The optical profiler consists of a microscope, an interferometer, a detector array, interface electronics, and a computer. While the basic theory for the optical profiler has been described previously [3], little was mentioned about the choice of interferometer. The optical interferometer used in the optical profiler depends on the magnification to be used. The Michelson interferometer shown in Fig. 1(a) is used for low magnifications of 1.5X, 2.5X, and 5X. An advantage of the Michelson interferometer is that only a single objective is needed. A disadvantage is that a beam splitter must be placed between the objective and the sample, so only objectives with long working distances can be used.

The Mirau interferometer shown in Fig. 1(b) is used for the medium magnifications of 10X, 20X, and 40X. The Mirau interferometer also has the advantage that only a single objective is required. While some optics must be placed between the objective and the sample, not as much working space is used up as for the Michelson. A disadvantage of the Mirau interferometer is that a central obscuration is present in the system. While this is not troublesome for a medium magnification, since the size of the obscuration is equal to the field of view of the sample, the obscuration becomes too large for low magnification systems.

The Linnik interferometer shown in Fig. 1(c) is used for the 100X, 150X, and 200X high magnification systems. It has the disadvantage that two matched objectives are required. However, since no optics are needed between the objective and the sample being measured, an objective with a large numerical aperture and a short working distance can be used.

Figure 2 shows an optical schematic of the optical profiler when the Linnik interferometer is attached. The light source is a tungsten halogen microscope illuminator. While different wavelengths can be selected using spectral filters, in most instances a spectral filter with a center wavelength of 650 nm and a passband of 40 nm is used. The 650 nm wavelength is a good compromise between the short wavelengths desired for optimum resolution and the long wavelengths for which the detector is optimized. The interference fringes can be viewed through the eyepieces. Also, the intensity of the interference fringes is read out using either a 256×256

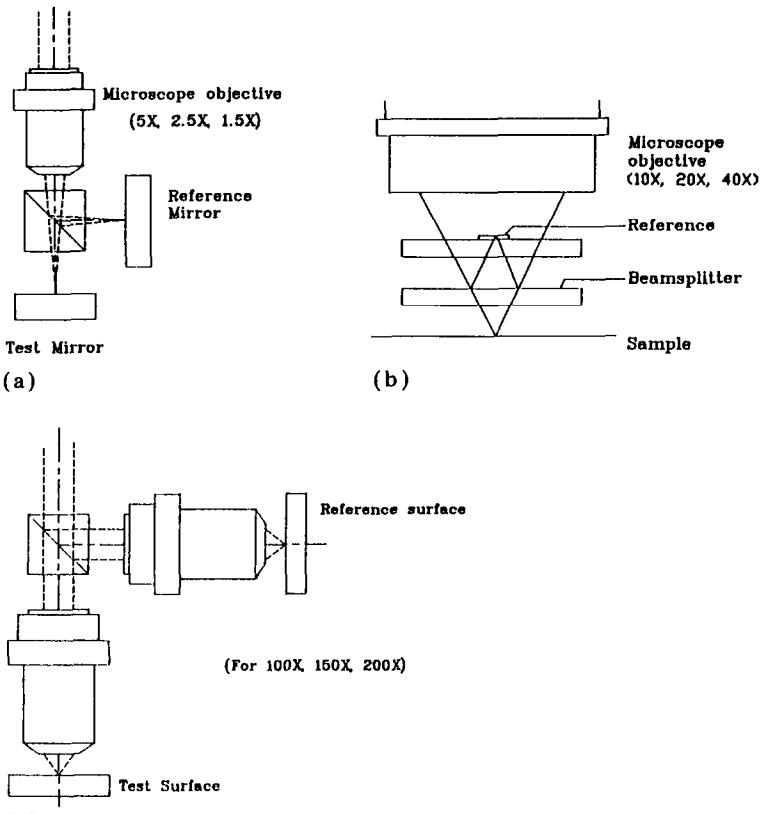

Fig. 1. Optical schematic of (a) Michelson interferometer, (b) Mirau interferometer, and (c) Linnik interferometer.

element photodiode array or a 1024 element linear charge-coupled device array. As shown previously [3], if the detector array is read out three or more times, and the reference mirror is moved approximately one-eighth wavelength between consecutive readouts, then the height variations across the test surface can be calculated. As shown in the figure, a piezoelectric transducer is used to move the reference mirror during the taking of the data.

Figure 3 shows a photograph of the optical profiler. The illuminator is to the left of the microscope. The Linnik interferometer is just above the sample mounted on the stage. The detector is in the cylindrical can at the top of the profiler. A linear profile is shown on the computer display.

Table 1 shows the optical profiler options. Listed for each magnification are the maximum profile length available, the spatial sampling interval, the optical resolution, the working distance, the maximum surface heights, and the maximum surface slopes that can be measured.

TABLE 1

Optical profiler options[a]

Objective magnification		1.5×	2.5×	5×	10×	20×	40×	100×	150×	200×
Interferometer type		Michelson	Michelson	Michelson	Mirau	Mirau	Mirau	Linnik	Linnik	Linnik
Profile length (mm)[b]	2D	8.87	5.32	2.66	1.33	0.666	0.333	0.133	0.089	0.067
	3D	6.8 × 6.8	4.1 × 4.1	2.0 × 2.0	1.0 × 1.0	0.5 × 0.5	0.25 × 0.25	0.1 × 0.1	0.068 × 0.068	0.05 × 0.05
Spatial sampling interval (μm)	2D	8.67	5.20	2.60	1.31	0.650	0.325	0.130	0.087	0.065
	3D	26.67	16.00	8.00	4.00	2.000	1.000	0.400	0.267	0.200
Working distance (mm)		11.5	1.5	1.5	4.5	2.5	4.0	1.0	0.2	0.2
Maximum surface heights (μm)		7.92	7.92	7.92	7.80	3.05	1.95	0.60	0.54	0.54
Maximum surface slopes (deg)	2D	0.81	1.34	2.69	5.37	10.74	21.49	48.12	53.85	53.85
	3D	0.26	0.44	0.87	1.75	3.49	6.98	17.46	26.19	34.91
Numerical aperture		0.0366	0.075	0.1	0.25	0.4	0.5	0.9	0.95	0.95
Optical resolution (μm)		10.83	5.29	3.97	1.59	0.99	0.79	0.44	0.42	0.42

[a] Vertical resolution (0.1 nm) unchanged for different magnifications.

[b] Profile length can be extended to several centimeters using a computer-controlled X–Y stage.

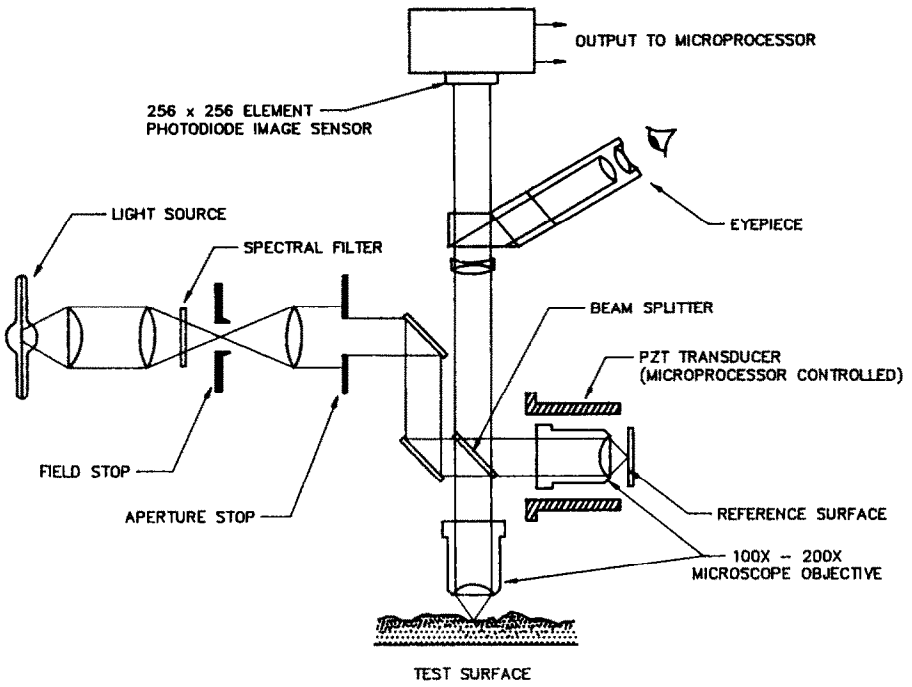

Fig. 2. Optical schematic of the three-dimensional digital optical profiler with Linnik interferometer.

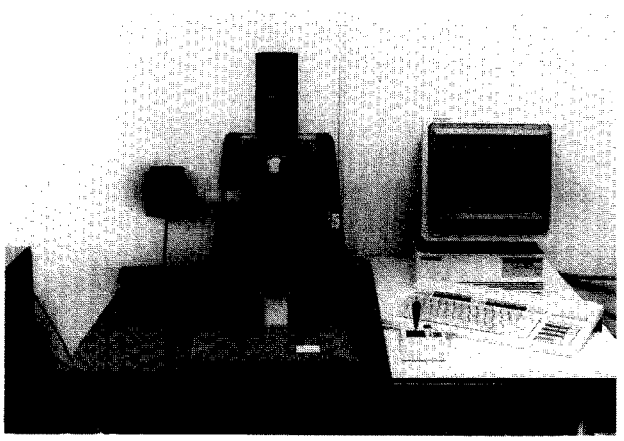

Fig. 3. Photograph of the optical profiler.

The two-dimensional profiler has detector elements spaced 13 μm apart and the three-dimensional profiler has detector elements spaced 40 μm apart. The maximum profile length is given by the number of detector elements (1024 for two dimensions and 256 for three dimensions) times the detector element spacing, divided by the magnification. The spatial sampling interval

is given by the detector element spacing, divided by the magnification. The optical resolution, which can be thought of as the closest that two features can be on the surface such that both features can be detected, is given by $0.61\lambda/(NA)$, where NA is the numerical aperture of the objective. In practice, because of aberrations in the optical system, the actual resolution is slightly worse than the optical resolution.

The working distance, which is the distance between the last element in the objective and the sample, is simply a characteristic of the particular objective used. The maximum surface height is given either by the coherence length of the source or by the depth of focus of the objective, whichever is shorter. For a 10× magnification or larger, the depth of focus sets the limit on the surface heights. The depth of focus, which is the depth region over which the image is sharp, is given by $\pm\lambda(1/2NA)^2$. The maximum surface slope is limited either by half the numerical aperture of the objective or by the slope such that between adjacent detector elements the height changes by one-fourth the wavelength of the light used in the measurement, whichever is smaller.

3. Data analysis

3.1. Surface topography statistics

Since much of the analysis software has been described previously [3], the description will not be repeated here. However, there are a few new features that need to be mentioned. The software will now calculate the arithmetic mean of the surface height variations as well as the peak-to-valley difference and the root mean square. Tilt of the surface and both spherical and cylindrical curvature can now be subtracted from the height data. If desired, the user can set the tilt of the surface. The radius of spherical curvature and cylindrical curvature can now be calculated. The height variations are now given in both metric and English units. Both autocovariance and power spectral density of the surface height variations are calculated. The three-dimensional maps can now be rotated and inverted. Typical measured results follow.

3.2. Geometrical parameters of a surface

Flatness, crown, camber, and twist of the rails (Fig. 4) of a magnetic slider can be measured using a low objective magnification. A magnification of 2.5× can view most of the slider. Three-dimensional or gray level plots are used to observe or measure these parameters. Taper angle can be measured by viewing the taper end of the rails at an objective magnification of 10× or higher.

Flatness. The greatest distance from a high or low point on a rail to a plane defined on the two rails is known as out of flatness.

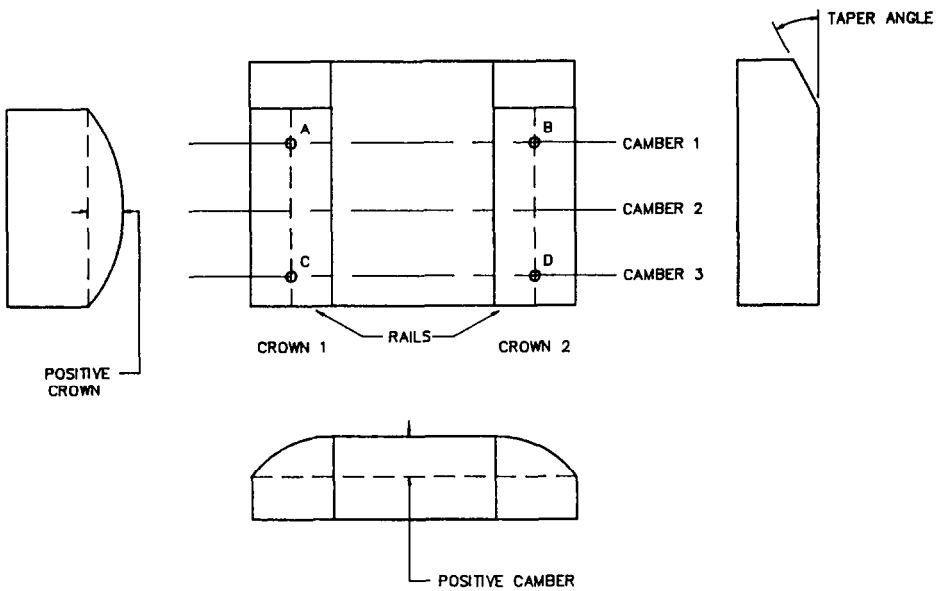

Fig. 4. Definitions of crown, camber, twist, and taper angle in a two-rail magnetic slider.

Crown. Crown is the distance between the highest (or lowest) point along a rail length and a line joining the end points of the rail. It is measured along the center of the rail width (Fig. 4).

Camber. Camber is the distance between the lines joining the inner and outer points along the rail width. It is measured at three locations on the rail.

Twist. When three out of four points on the rail (A, B, C, D in Fig. 4) form a plane, the twist is the vertical distance between the fourth point and the plane. If the fourth point is above the plane, twist is positive. Twist is also defined by a distance obtained by multiplying the rail length by the angle between the planes of the two rails.

Taper angle. Taper angle is the angle the taper of the slider forms with the rail (Fig. 4).

4. Results and discussion

The profiler can be used at objective magnifications of 1.5X, 2.5X, 10X, 20X, 40X, 100X, 150X, and 200X. Table 2 shows the results of measurements made on a computer tape (the same as that used in ref. 3) at 20X through 200X magnifications. It should be noted that the measured values are different at various magnifications because of differences in pixel spacing. Typical surface plots and profiles at objective magnifications of 20X and 200X are shown in Fig. 5. Significantly more topographical detail can

TABLE 2

Surface topography statistics of magnetic tape A from three-dimensional optical profiler at various objective magnifications

	20X	*40X*	*100X*	*150X*	*200X*
R.m.s. surface height (nm)	22.4	19.5	20.9	18.0	17.1
R.m.s. profile slope x (mrad)	2.2	3.6	7.8	17.1	21.9
R.m.s. profile slope y (mrad)	1.8	3.2	7.1	18.6	24.5
Mean surface slope (mrad)	2.3	4.2	9.0	21.7	27.6
Standard deviation surface slope (mrad)	2.8	4.8	10.5	25.3	32.8
R.m.s. profile curvature x (mm^{-1})	0.83	3.9	22.6	76.9	119.0
R.m.s. profile curvature y (mm^{-1})	0.62	2.9	15.8	72.9	114.3
R.m.s. surface curvature (mm^{-1})	0.54	2.5	14.2	54.2	85.2
Summit height[a] (nm)					
Mean	23/35	11/19	8/26	10/17	11/20
Standard deviation	25/21	19/14	24/12	17/12	15/10
Summit slope[a] (mrad)					
Mean	1.2/1.4	2.2/2.2	5.2/5.6	13.1/13.7	15.9/16.7
Standard deviation	1.0/1.0	1.0/1.1	2.4/2.0	5.4/5.4	6.4/6.4
Summit curvature[a] (mm^{-1})					
Mean	1.6/1.6	6.4/6.6	40.0/41.0	116.5/118.8	179.3/183.3
Standard deviation	0.8/0.9	2.2/2.4	14.0/15.0	38.1/40.3	55.8/59.8
Summit-to-valley distance (nm)	324	162	143	171	245
Number of summits per square millimeter[a]	370/ 233	5674/ 4309	24287/ 13414	191400/ 142900	180100/ 118700
Profile zero crossings x (mm^{-1})	28	44	110	226	483
Profile zero crossings y (mm^{-1})	20	29	94	251	439
Surface zero crossings (mm^{-1})	99	100	182	285	400
Average autocorrelation distance (μm)	21	20	11	7	5
Anisotropy ratio	3.4	2.7	1.5	1.4	1.1

[a]Mean and standard deviation are given for all summits (first numbers) and top 25% of all summits (second numbers).

be seen at 200X compared with 20X. Since finer asperities and valleys can be seen at higher magnifications, surfaces appear to have higher slope, curvature, summit slope, summit curvature, summit density, and a higher number of zero crossings. Since finer details of topography can be detected at higher magnifications, the autocorrelation distance is smaller and the surface appears to be more isotropic (Fig. 6).

The radius and surface roughness of cylindrical and spherical surfaces can also be measured. A surface profile of a 2 in ball-bearing with and without radius is shown in Fig. 7(a). Radius can be measured by this instrument with a very high accuracy. A diamond-turned cylinder is shown in Fig. 7(b). Figure 8 shows examples of a scratch on a disk surface measured at 200X magnification.

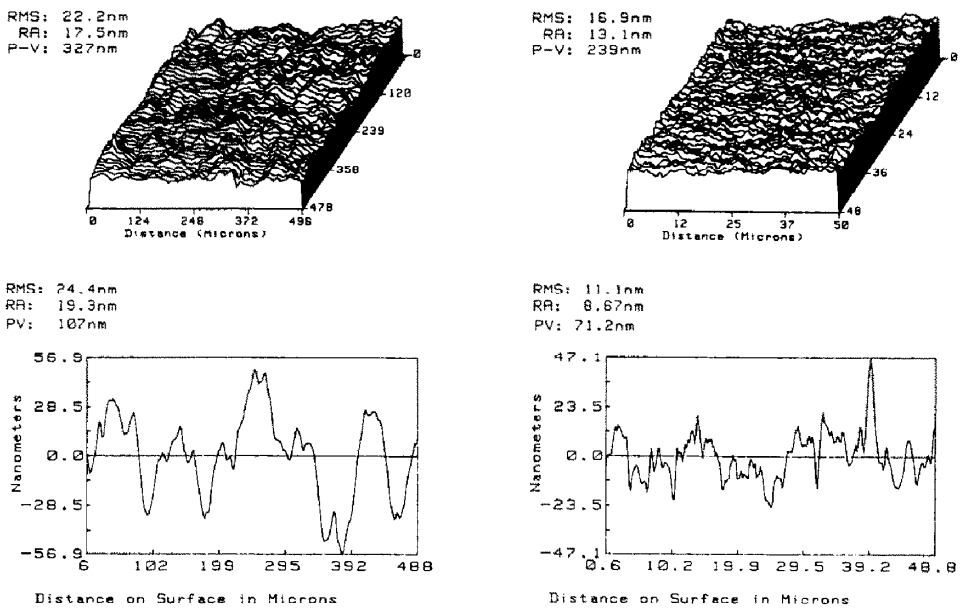

(a) (b)

Fig. 5. Three-dimensional surface and two-dimensional profile plots of tape A measured at (a) 20× and (b) 200×.

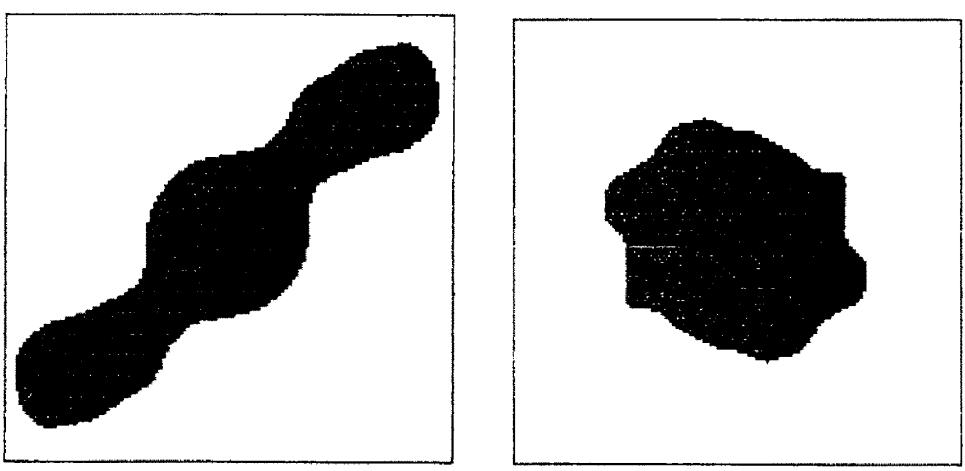

(a) (b)

Fig. 6. Plot showing the points for which the autocovariance is greater than 0.1 for tape A measured at (a) 20× and (b) 200×.

Three-dimensional profiles of two rails on a slider are shown in Fig. 9(a). By measuring profiles along and across the rails (*e.g.* Figs. 9(b) and 9(c)) crown, camber, and twist can be determined. The condition of the edges

of rails can be found from the three-dimensional plot in Fig. 9(a). The taper angle is measured from the profile of the taper end of the rail along the rail at 10X objective magnification (Fig. 10).

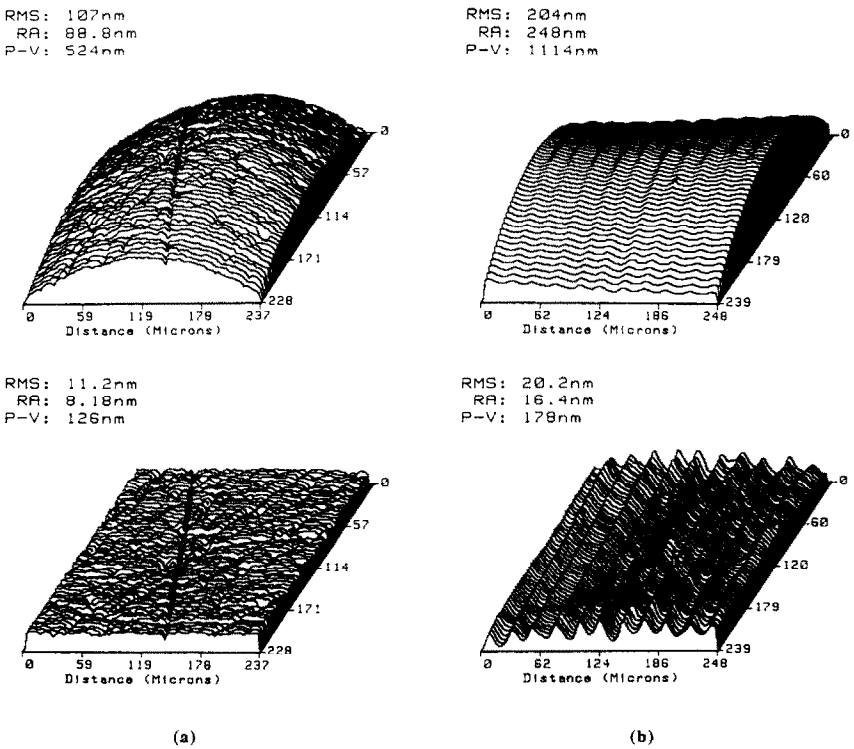

Fig. 7. Three-dimensional surface plot at 40X of (a) a 2 in ball-bearing with radius (top) and radius subtracted from the profile (bottom). (b) A diamond-turned cylinder with radius (top) and radius subtracted from the profile (bottom). Radius of the cylinder is 6.76 mm.

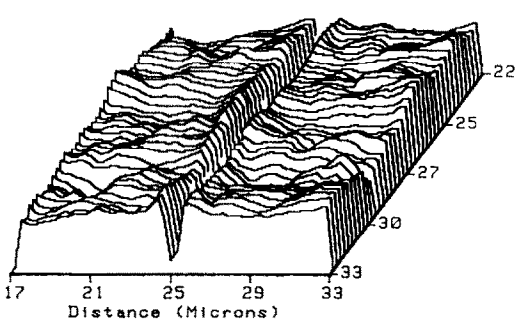

Fig. 8. Three-dimensional surface plot of a magnetic disk at 200X showing a scratch.

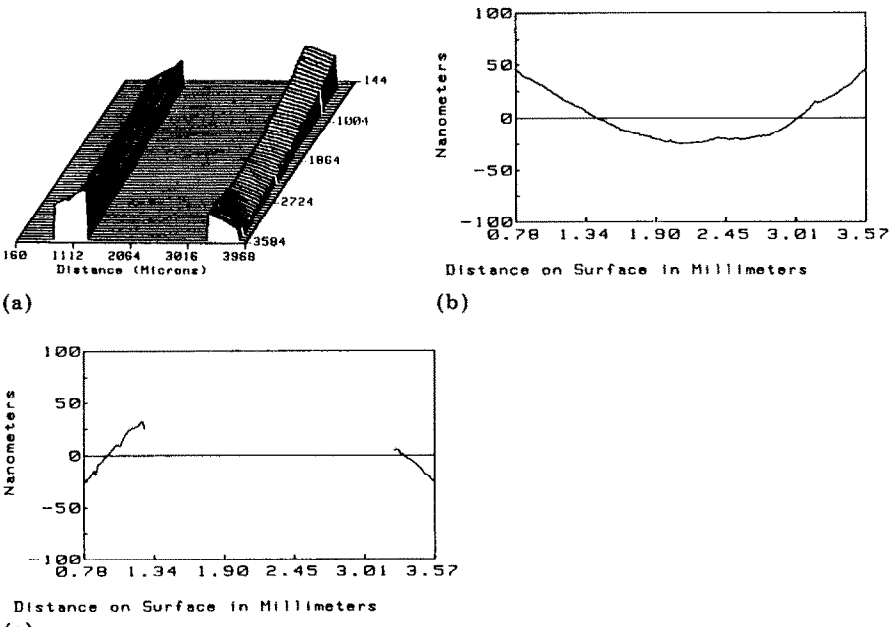

Fig. 9. (a) Three-dimensional surface plot of a magnetic slider at 2.5× (taper area not shown). (b) Profile along a rail length. (c) Profile across the two rails. Crown 1,97 nm; crown 2,66 nm; camber 1,55 nm; camber 2,55 nm; camber 3,57 nm; twist, 162 nm; out of flatness, 223 nm.

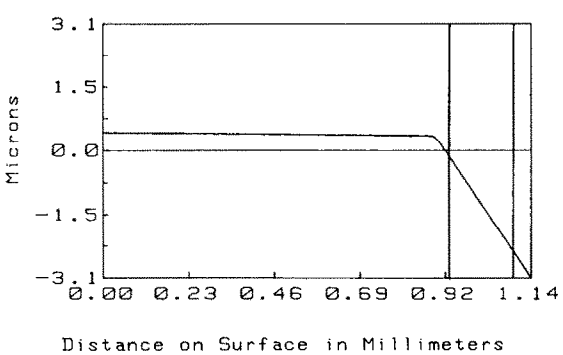

Fig. 10. Profile of the taper end of the slider rail along the rail length at 10×. Taper angle is 13.4 mrad.

An example of the pole-tip gap recession is shown in Fig. 11(a). The three-dimensional plot is inverted to give a better view of the recession area shown in Fig. 11(b).

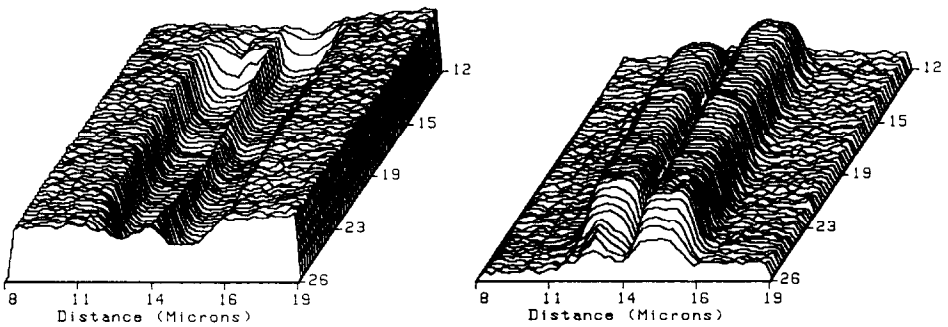

(a) (b)

Fig. 11. Three-dimensional surface plot of pole-tip gap recession in magnetic slider at 200×. (a) recession profile and (b) recession profile inverted.

References

1 T. R. Thomas, *Rough Surfaces*, Longman, London, 1982.
2 B. Bhushan, J. C. Wyant and C. L. Koliopoulos, Measurement of surface topography of magnetic tapes by Mirau interferometry, *Appl. Opt.*, *24* (1985) 1489 - 1497.
3 J. C. Wyant, C. L. Koliopoulos, B. Bhushan and D. Basila, Development of a three-dimensional noncontact digital optical profiler, *J. Tribol.*, *108* (1986) 1 - 8.